

# Palaeomagnetic analyses of calcified deposits from the Plio-Pleistocene hominid site of Kromdraai, South Africa

J.F. Thackeray<sup>a†</sup>, Joseph L. Kirschvink<sup>b,c</sup> and Timothy D. Raub<sup>b,†</sup>

**P**ALAEOMAGNETIC DATA ARE PRESENTED for a set of orientated cores from a talus cone at Kromdraai B, a South African cave deposit associated with early Pleistocene fauna including important hominid remains of *Paranthropus (Australopithecus) robustus*. Polarity interpretations of calcified sediments and flowstones suggest that the cave deposits include episodes of deposition that span the Olduvai Event of the Matuyama chron. Results suggest that matrix of the kind associated with the type specimen of *P. robustus* (TM 1517) corresponds closely to the beginning of the Olduvai Event, c. 1.9 Myr ago.

Kromdraai B, situated approximately 2 km east of Sterkfontein in Gauteng, South Africa (26°00'0"S, 27°45'0"E), yielded the first specimen of *Paranthropus (Australopithecus) robustus*.<sup>1,2</sup> On the basis of faunal associations and correlations with East African sequences dated with K/Ar and magnetostratigraphy, Kromdraai B deposits are considered to date between 1.5 and 2.0 million years ago (Myr).<sup>3-6</sup> The type specimen of *P. robustus* (TM 1517), discovered in 1938, and other specimens from this site,<sup>7</sup> are morphologically similar to 'robust' australopithecines from East Africa, including the '*Zinjanthropus*' cranium discovered by Mary and Louis Leakey in Bed 1 at Olduvai Gorge in Tanzania, and described by Tobias<sup>8</sup> as *Australopithecus boisei*.

The type locality of *P. robustus* is referred to as Kromdraai B, distinct from Kromdraai A, the so-called 'faunal' site situated 30 m west of Kromdraai B, containing stone artefacts described as Oldowan and Acheulean.<sup>9</sup> Unfortunately, it is not known exactly where the type specimen

of *P. robustus* was discovered at Kromdraai, but grey matrix of the kind associated with the fossil predates a calcium carbonate flowstone that is represented on the eastern margin of the KB site, between 37 and 38 m east of datum.

Previous palaeomagnetic analyses on Kromdraai B deposits were attempted by Jones *et al.*<sup>10</sup> Some of their breccia samples showed reversed polarity, but most of the results were 'intermediate' between reversed and normal polarity, and as such are of uncertain value. More reliable are analyses on calcite and flowstone deposits, as demonstrated for Sterkfontein deposits.<sup>11</sup> Recently, orientated cores from Kromdraai B have been sub-sampled and analysed for palaeomagnetic stability at the California Institute of Technology. In this study, we present new palaeomagnetic data for flowstone and calcified deposits from Kromdraai B in an attempt to place magnetic polarity constraints on deposits that have yielded fossils.

## Methods

With permission from the South African Heritage Resources Agency, we collected 12 orientated samples from Kromdraai B with a portable, petrol-powered drill using a non-magnetic, 2.5-cm-diameter, diamond-tipped coring tube. To minimize damage to the outcrop, care was taken to drill as deeply as possible (typically between 5 and 10 cm) perpendicular to the layering of the flowstones and any obvious bedding. In turn, these cores were sub-divided into as many specimens approximately 1 cm high as the length of the core would permit, for a total of 59 orientated specimens. After preparation, all specimens were rinsed briefly in 0.5 N HCl to remove any surface contaminants from the drilling and sub-sampling procedures, labelled with ceramic ink, and stored for several weeks in a magnetically shielded room to allow for the decay of viscous magnetic components. Measurements of the natural remanent magnetism (NRM) were made with a 3-axis 2G Enterprises™ moment

magnetometer using d.c.-biased superconducting quantum interference device (SQUID) detectors, coupled with a custom-built computer-controlled vacuum pick-and-put sample changing system. All specimens were subjected to initial magnetic cleaning in low-intensity alternating magnetic fields (A.f. demagnetization), in 2-mT steps to a maximum of 10 mT, principally to remove any lingering magnetization that may have been produced by lightning strikes, airport X-ray machines or other sampling artifacts. They were then subjected to progressive thermal demagnetization at 75, 150 and 200°C steps, then at additional 25°C intervals until their magnetizations either became unstable, became too weak to measure reliably (<10<sup>-11</sup> Am<sup>2</sup>), or else revealed no further magnetic components. Complete duplicate measurements (both up- and down-arrow with four independent readings per axis) were measured after each thermal demagnetization step. The complete data set contains nearly 900 such discrete measurements, about 15 per specimen. Data were subject to principal component analysis,<sup>12</sup> with maximum MAD values for least-squares lines and planes of 10 and 15 degrees, respectively, and a joint line-and-plane analysis was conducted using the technique of McFadden and McElhinny.<sup>13</sup> Small samples of representative lithologies were subjected to a battery of rock-magnetic experiments including ARM and IRM acquisition, and A.f. demagnetization to characterize the magnetic minerals present.

## Results

Results of our analyses are summarized in Table 1. Figure 1 shows three representative sets of demagnetization data, including one clearly reversed specimen (KBM 11.1), and two others of probable normal polarity (KBM 3.1 and 2.2). Figure 2 shows least-squares results from these analyses, and a summary is given in Table 1. The contextual information includes depth below datum and metres north and east of the datum. Results from sample KBM-2, in which the base and top of the core record different magnetic polarities, are shown in Fig. 3. Results of a rock-magnetic analysis on a lithological sample from core KBM-9 are given in Fig. 4. Figure 5 illustrates a stratigraphic sequence with a flowstone (FS), represented by KBM samples 7 and 8, overlying grey breccia and underlain by a red breccia (RB) represented by sample KBM 6.

## Discussion and conclusion

Any palaeomagnetic study of young, undeformed sediments suffers some uncertainty in distinguishing specimens of normal polarity, magnetized soon after

<sup>a</sup>Transvaal Museum, P.O. Box 413, Pretoria 0001, South Africa.

<sup>b</sup>Division of Geological and Planetary Sciences, 170-25, California Institute of Technology, Pasadena, CA 91125, U.S.A.

<sup>c</sup>Department of Earth and Planetary Science, Graduate School of Science, University of Tokyo 7-3-1 Hongo, Bunkyo-ku, Tokyo 113-0033, Japan.

<sup>†</sup>Author for correspondence.

E-mail: mrspl@global.co.za.

<sup>‡</sup>Present address: Department of Geology and Geophysics, Yale University, P.O. Box 208109, New Haven, CT 06520-8109, U.S.A.

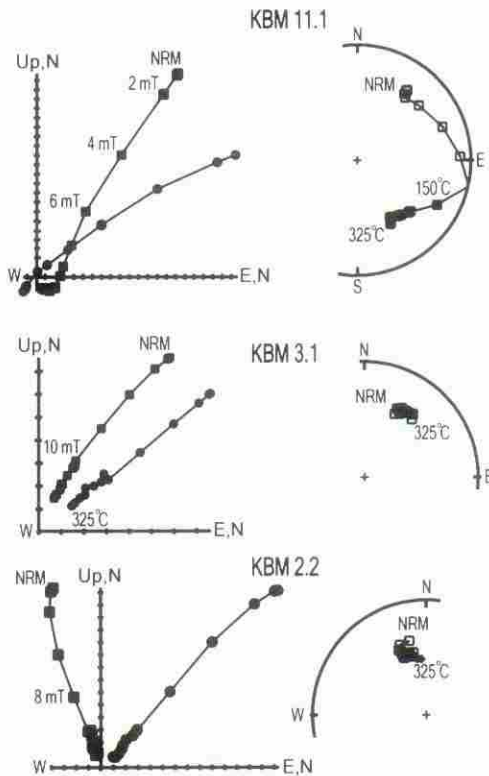


**Fig. 1.** Representative demagnetization behaviour of specimens from Kromdraai site B (located at  $26^{\circ}00'0''S$ ,  $27^{\circ}45'0''E$ ). Specimen KBM 11.1 is interpreted to be reversely magnetized because it shows a great circle arc that terminates in a 'south and down' direction. Samples KBM 2.2 and 3.1 show interpreted normal polarity characterized by a stable, northerly and upwards direction distinct from the present local field. On the equal-area projections, open (filled) symbols represent upper (lower) hemisphere directions. For the orthogonal projections, squares show the projection into the horizontal plane, and circles into the vertical, north-south plane.

deposition, from specimens remagnetized by recent weathering or viscous relaxation of magnetic minerals. By contrast, reversed polarities can usually be identified reliably by large directional shifts during progressive demagnetization experiments (for example, specimen KBM 11.1 in Fig. 1) or by trends of smaller, great-circle arcs leading towards reversed directions (for example, specimens KBM 2.5 and 2.6 shown in Fig. 3). Sedimentary breccias and flowstones at Kromdraai and Sterkfontein are no exception. As shown in Fig. 4, detrital antiferromagnetic minerals (principally fine-grained goethite and haematite) and, to some degree, their fer-

romagnetic counterparts (magnetite and maghaemite) may be incorporated in syndepositional cave talus breccias. While these minerals, which give the matrix its reddish colour, do preserve a primary magnetization, they may be altered and dehydrated in time as well, forming magnetic overprints. The hybrid demagnetization strategy employed here (low alternating fields followed by thermal demagnetization) specifically is aimed at removing soft viscous components from multi-domain particles and finer-grained secondary pigment minerals of low magnetic stability. The demagnetization of specimen KBM 11.1 (Fig. 1, top) illustrates

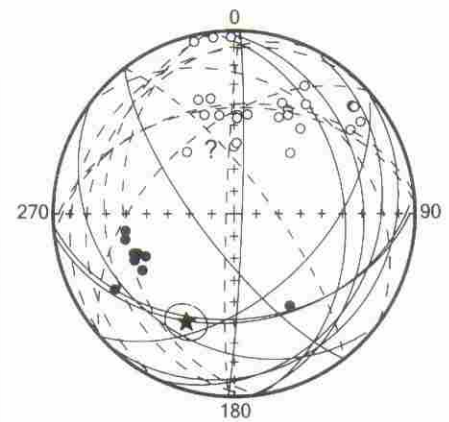


**Fig. 2.** High-stability, least-squares directions for the principal (and possibly primary) magnetic components from all KBM specimens. The question mark (?) gives the direction of the present local field (on the upper hemisphere) and indicates some uncertainty in the interpretation of polarity results for directions that fall in the vicinity. Open circles indicate line directions on the upper hemisphere (negative inclinations of normal polarity), whereas filled symbols lie on the lower hemisphere (reversed polarity). Great-circle arcs (dotted on the upper hemisphere) indicate the locus of demagnetization planes for reverse-magnetized specimens that do not clean up completely to yield a demagnetization line. The black star is the mean of analyses, calculated using the statistics of McFadden and McElhinny,<sup>13</sup> with each specimen given unit weight. Statistics based on 36 lines and 10 great circles (planes) are:  $D, I = (204.2, 35.0)^{\circ}$ ,  $\kappa = 6.7$ ,  $\alpha_{95} = 8.7^{\circ}$ ,  $R = 39.33$ ,  $S = 29.7$ . Note that we do not assign any tectonic significance to the deviation of this mean direction from the local geocentric axial dipole direction, as the intent which guided our sampling strategy in the field was to constrain fossil locations with magnetostratigraphy, not to obtain a pole position.

just how pervasive this remagnetization can be, as roughly 90% of the natural remnant magnetization is removed by the low-field A.f. and first thermal steps before an underlying reversed component is revealed. Unfortunately, the carbonate matrix limits the temperature range over which useful data may be recovered due to thermal decarboxylation reactions.

Nevertheless, 46 out of 59 specimens from Kromdraai B yield results that are both sufficiently distant from the present field direction ( $D, I = -17.6^{\circ}, -63.5^{\circ}$ ) to rule out remagnetization in the past few hundred years, and sufficiently stable and consistent in NRM to guide recognition of principal-component lines and planes, as in Fig. 2. Although scatter in the data exceeds that expected from natural secular variation processes, all specimens but one (which possibly contains a magnetic clast) divide easily into 'reversed' and 'possibly normal' groups. We exclude all specimens belonging to samples KBM 9 and 10 from polarity interpretation as their remanence sits on the same direction through the entire demagnetization process, and have probably been subjected to

**Table 1.** Results obtained from orientated core samples from a talus cone at Kromdraai B.

Sample	Metres north of datum	Metres east of datum	Metres below datum	Polarity
KBM 2	2.0	34.0	0.9	Transition from normal (base of core) to reversed polarity (top of core)
KBM 3	3.1	35.2	1.0	Normal
KBM 4	3.3	35.4	1.1	Normal
KBM 5	3.1	36.0	0.9	Normal
KBM 6	1.4	36.9	0.6	Normal
KBM 12	2.2	33.6	1.5	Normal
KBM 1	2.1	33.7	1.4	Reversed
KBM 7	1.7	37.4	0.7	Reversed
KBM 8	1.7	38.1	0.9	Reversed
KBM 11	2.5	34.4	1.1	Reversed
KBM 9	2.7	33.9	1.0	Inconclusive
KBM 10	2.5	34.1	1.0	Inconclusive

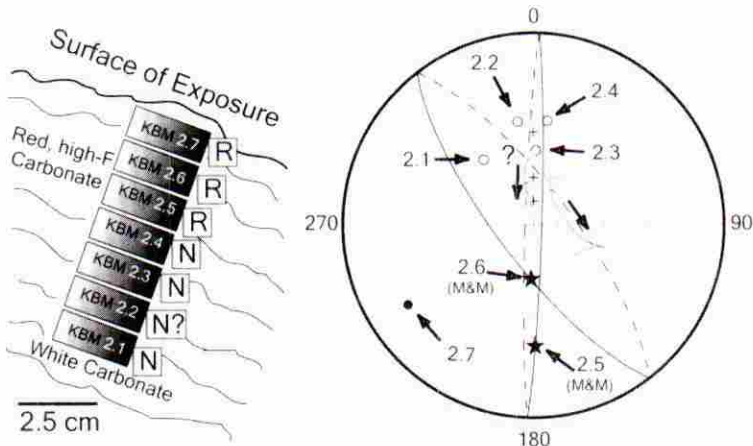


**Fig. 3.** Results of progressive demagnetization of seven specimens from sample KBM 2, with a sketch of their relative position and orientation in the flowstone at the margin of the growing talus pile. Note that the first four specimens (2.1–2.4) yielded normal directions (north and up). Specimens 2.5 and 2.6 produced data aligned along great-circle arcs (demagnetization planes), data shown as the string of thinner circles connected by a central line. The direction of motion with increasing demagnetization is indicated by the arrows, along with the two great circles of best least-squares fit. Symbols are as used in Fig. 2. The best-guess characteristic directions for these two specimens, based on the iterative statistics of McFadden and McElhinny,<sup>13</sup> are shown by two black stars on these great-circle paths, labelled KBM 2.5 and 2.6, M&M. Thus, the top three specimens indicate reverse polarity. There is also a great difference in magnetic intensity between these specimens. The first specimen (2.1), a white carbonate, is the furthest into the hole and also the weakest. A few centimetres out of the bottom of the hole, magnetic intensity increases by a factor of nearly 100 and ultimately nearly 1000 times (in the reddish layer of specimen (2.5) before returning to typical values near the surface of the hole. These intensity variations do not seem to be correlated with direction or polarity.

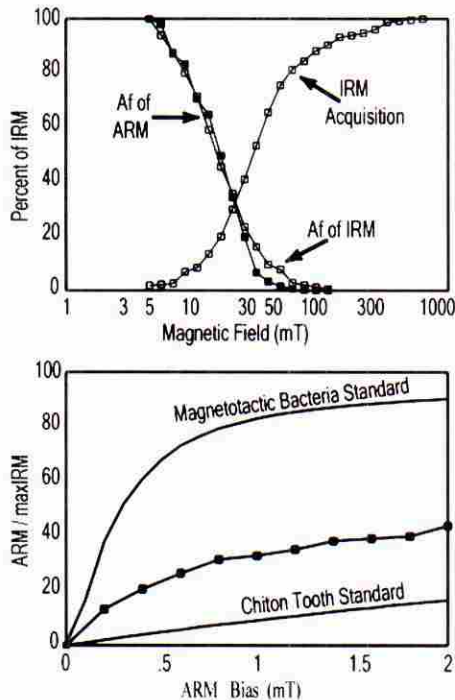


**Fig. 4.** Rock magnetic data from sample KBM 9. All specimens yield characteristic directions parallel to the present local geomagnetic field. The top diagram shows results of coercivity spectra analysis, including alternating-field (A.f.) demagnetization of anhysteretic remanent magnetization (ARM, filled squares), given in a 100-mT peak field with a 2-mT d.c. bias. This is compared with A.f. demagnetization of a 100-mT isothermal remanent magnetization (IRM, open squares), and an IRM acquisition experiment under increasing pulse fields up to 1000 mT.<sup>17,18</sup> The observation that most specimens gain or lose their magnetization in fields below 300 mT argues against the presence of high concentrations of large antiferromagnetic minerals (like haematite and goethite), although an observed slight increase in moment above this level is consistent with some fine-grained antiferromagnetic pigments. The drop in the A.f. of ARM curve with respect to the A.f. of IRM curve between 30 and 80 mT suggests the presence of some multi-domain material (partially oxidized magnetites?). The bottom graph traces acquisition of ARM in the specimen, exposed to progressively stronger d.c. biasing fields up to 2 mT, compared to reference curves for freeze-dried magnetotactic bacteria and the tooth of a chiton, *Polyplacophoran mollusk*. These data indicate a significant fraction of finely dispersed magnetic pigments (presumably ferromagnetic oxides) that interact magnetically with each other only marginally.

remagnetization.

Given these considerations, specimens from core-samples KBM 3, 4, 5, and 6 are all associated with normal polarity. These samples may represent part of a penecontemporaneous talus cone covering deposits represented by samples KBM 1, 7 and 8, which all display reversed polarity. KBM 7 and 8 were sampled from a flowstone deposit overlying grey matrix of the kind associated with TM 1517.

As shown in Fig. 3, KBM 2 indicates a surfaceward transition from normal to reversed polarity. This pattern argues still further against chemical remagnetization, as by leaching, in this sample.

Recognizing that the Kromdraai B fauna are thought to fall within the 2.0–1.5 Myr window,<sup>3,4</sup> we suggest provisionally that samples KBM 1, 7 and 8 relate to an interval of reversed polarity, c. 2.0 Myr ago, prior to the Olduvai Event; that samples KBM 3, 4, 5 and 6 relate to the period of normal polarity within the Olduvai interval of 1.95–1.77 Myr.<sup>14</sup> Sample KBM 2 may perhaps record the end of the Olduvai Event, showing a transition from normal to reversed polarity. Younger breccia may be represented in adjacent deposits, including material analysed using electron spin resonance.<sup>15</sup>

Five lithostratigraphic members have been identified from a study of cores drilled at Kromdraai B.<sup>3,16</sup> Most, if not all, of the samples that we have analysed relate to Members 1 and 2 on the eastern side of Kromdraai B, but the distinction between these two members is not clear. However, the grey breccia, underlying a flowstone layer represented by samples KBM 7 and 8 (Fig. 5), is of the kind associated with TM 1517, the type specimen of *P. robustus*. We infer that the type specimen and penecontemporaneous hominids from Kromdraai are probably associated with an episode of deposition close in time to the beginning of the Olduvai Event, c. 1.9 Myr ago.

We are grateful to the South African Department of Arts, Culture, Science and Technology, associated with the Palaeoanthropological Heritage Project, and the National Research Foundation, for supporting palaeontological research at Kromdraai. We also thank Francis MacDonald for assistance in the laboratory, Lawrence Radebe for help in the field, and T.C. Partridge for helpful comments. We gratefully acknowledge the use of the *Palcomac* software package of J.P. Cogne of the IPGP in Paris, available at <http://www.ipgp.jussieu.fr/~cogne>.

1. Broom R. and Schepers G.W.H. (1946). *The South African ape-men: the Australopithecinae*. Transvaal Museum Memoir No. 2. Pretoria.
2. Brain C.K. (1981). *The Hunters or the Hunted? An introduction to African Cave Taphonomy*. University of Chicago Press, Chicago.
3. Vrba E.S. and Panagos D.C. (1982). New perspectives on taphonomy, palaeoecology and chronology of the Kromdraai ape-man. In *Palaeoecology of Africa and the Surrounding Islands*, eds I.A. Coetzee and E.M. van Zinderen Bakker, 15, 13–26.

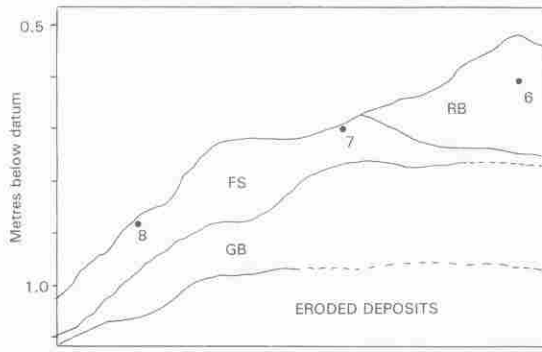


**Fig. 5.** Simplified section of calcified deposits at Kromdraai B, between 37 and 38 m east of datum, and between 0.5 and 1.0 m below datum. GB: Grey breccia; FS, flowstone; RB, red breccia. Sample KBM 6 (normal polarity) overlies samples KBM 7 and 8 (reversed polarity).

4. Vrba E.S. (1985). Early hominids in southern Africa: updated observations on chronological and ecological background. In *Hominid Evolution, Past Present and Future*, ed. P.V. Tobias, pp. 195–200. Alan R. Liss, New York.
5. Vrba E.S. (1985). Ecological and adaptive changes associated with early hominid evolution. In *Ancestors, The Hard Evidence*, ed. E. Delson, pp. 63–71. Alan R. Liss, New York.
6. Delson E. (1988). Chronology of South African australopithecine site units. In *Evolutionary History of the "Robust" Australopithecines*, ed. E.E. Grine, pp. 317–324. A. de Gruyter, New York.
7. Thackeray J.F., de Ruiter D.J., Berger L.R. and van der Merwe N.J. (2001). Hominid fossils from Kromdraai: a revised list of specimens discovered since 1938. *Ann. Transv. Mus.* **38**, 43–56.
8. Tobias P.V. (1967). *The Cranium and Maxillary Dentition of Australopithecus (Zinjanthropus) boisei*. Olduvai Gorge, vol. 2. Cambridge University Press, Cambridge.
9. Kuman K., Field A.S. and Thackeray J.F. (1997). Discovery of new artefacts at Kromdraai. *S. Afr. J. Sci.* **93**, 187–193.
10. Jones D.L., Brock A. and McFadden P.L. (1986). Palaeomagnetic results from the Kromdraai and

11. Partridge T.C., Shaw J., Heslop D. and Clarke R.J. (1999). The new hominid skeleton from Sterkfontein, South Africa: age and preliminary assessment. *J. Quat. Sci.* **14**, 293–298.
12. Kirschvink J.L. (1980). The least-squares line and plane and the analysis of paleomagnetic data: examples from Siberia and Morocco. *Geoph. J. R. Astr. Soc.* **62**, 699–718.
13. McFadden P.L. and McElhinny M.W. (1988). The combined analysis of remagnetization circles and direct observations in paleomagnetism. *Earth Planet. Sci. Lett.* **87**, 161–172.
14. Tamrat E., Thouveny N., Taieb M. and Opdyke N.D. (1995). Revised magnetostratigraphy of the Plio-Pleistocene sedimentary sequence of the Olduvai Formation (Tanzania). *Palaeogeog., Palaeoclimat., Palaeoecol.* **114**, 273–283.
15. Curnoe D., Grün R. and Thackeray J.F. (2002). Electron spin resonance dating of tooth enamel from Kromdraai B, South Africa. *S. Afr. J. Sci.* **98**, 540.
16. Partridge T.C. (1982). Some preliminary observations on the stratigraphy and sedimentology of the Kromdraai B hominid site. In *Palaeogeology of Africa and the Surrounding Islands*, eds J.A. Coetzee and E.M. van Zinderen Bakker, **15**, 3–12.
17. Chang S.-B.R. and Kirschvink J.L. (1989). Magnetofossils, the magnetization of sediments, and the evolution of magnetite biomineralization. *Ann. Rev. Earth Planet. Sci.* **17**, 169–195.
18. Cisowski S. (1981). Interacting vs. non-interacting single-domain behavior in natural and synthetic samples. *Phys. Earth Planet. Interiors* **26**, 56–62. □

## Electron spin resonance dating of tooth enamel from Kromdraai B, South Africa

D. Curnoe<sup>a\*</sup>, R. Grün<sup>b</sup> and J.F. Thackeray<sup>c</sup>

**E**LECTRON SPIN RESONANCE (ESR) DATING offers the potential to provide dates for Plio-Pleistocene sites in South Africa. Previous attempts have been made to date tooth enamel samples from Sterkfontein, Swartkrans and Gladysvale.<sup>1–4</sup> Here we report results of ESR dating of tooth enamel from Kromdraai B in the Sterkfontein Valley.

A single bovid tooth was recovered from a block of breccia excavated in July 1995 and catalogued as KB 193. The breccia is stratigraphically younger than a flowstone that was dated to the early Pleistocene using palaeomagnetic dating in combination with faunal associations and biostratigraphy.<sup>5</sup>

The basic principles of ESR dating have recently been reviewed.<sup>6–8</sup> In this study, sample preparation and measurements followed conventional ESR procedures.<sup>9</sup> ESR spectra were analysed using peak-to-peak measurements, dose versus magnetic field plots, and spectrum deconvolution with four Gaussian curves.<sup>10–12</sup>

The results are as follows: a weighted average date of  $568 \pm 27$  kyr was obtained from the early uranium uptake (EU) model, and  $814 \pm 32$  kyr from the linear uptake (LU) model. The difference between the EU and LU age estimates is large, due to the relatively high concentrations of uranium in enamel and dentine. We therefore undertook isochron estimates,<sup>13</sup> which provided an age for the tooth of 668 kyr (errors were highly correlated and cannot be reliably determined). Some of the difficulties associated with ESR dating of Pliocene and early Pleistocene fossils from South African cave deposits may be overcome through careful collection of *in situ* tooth and sediment samples. Additional analyses, particularly U-series measurements of enamel and dentine, can be expected to reduce dating uncertainties.<sup>7,8</sup> However, the reliable assessment of external dose rates within the context of complex stratigraphy and depositional sequences, and unknown geochemical histories, remains a major challenge.

We thank the National Research Foundation, the Australian National University, and Department of Employment (Training and Youth Affairs) for support. We also thank L. Taylor for chemical analyses, T. Prior for access to irradiation facilities at the CSIRO

Black Mountain Laboratories in Australia, and L. Radebe for assistance in the field.

1. Curnoe D. (1999). *A contribution to the question of early Homo in southern Africa*. PhD thesis, Australian National University, Canberra.
2. Blackwell B. (1994). Problems associated with re-worked teeth in electron spin resonance (ESR) dating. *Quaternary Geochronology (Quaternary Science Reviews)* **13**, 651–660.
3. Schwartz H.P., Grün R. and Tobias P.V. (1994). ESR dating of the australopithecine site of Sterkfontein, South Africa. *J. Hum. Evol.* **26**, 175–181.
4. Curnoe D., Grün R., Taylor L. and Thackeray J.F. (2001). Direct ESR dating of a Plio-Pleistocene hominid from Swartkrans. *J. Hum. Evol.* **40**, 379–391.
5. Thackeray J.F. and Kirschvink J.L. and Traub T.B. (2002). Palaeomagnetic analyses of calcified deposits from the Plio-Pleistocene hominid site of Kromdraai, South Africa. *S. Afr. J. Sci.* **98**, 537–540.
6. Grün R. (1997). Electron spin resonance dating. In *Chronometric and Allied Dating in Archaeology*, eds R.E. Taylor and M.J. Aitkens, pp. 217–261. Plenum, New York.
7. Grün R. (2000). Electron spin resonance dating. In *Modern Analytical Methods in Art and Archaeology*. Chemical analyses series 155, eds E. Ciliberto and G. Spoto, pp. 641–679. Wiley, New York.
8. Grün R. (2000). Dating beyond the radiocarbon barrier using U-series isotopes and trapped charges. In *Radiation in Art and Archaeometry*, eds D.C. Creagh and D.A. Bradley. Elsevier, Amsterdam.
9. Grün R. (1989). Electron spin resonance (ESR) dating. *Quat. Int.* **1**, 65–109.
10. Grün R. (1998). Dose determination on fossil tooth enamel using spectrum deconvolution with Gaussian and Lorentzian peak shapes. *Ancient TL* **16**, 51–55.
11. Grün R. (2000). Methods of dose determination using ESR spectra of tooth enamel. *Radiation Measurements* **32**, 767–772.
12. Robertson S. and Grün R. (2000). Dose determination on tooth enamel fragments from two human fossils. *Radiation Measurements* **32**, 773–779.
13. Blackwell B.A. and Schwartz H.P. (1993). ESR isochron dating of teeth: a brief demonstration in solving the external dose calculation problem. *Appl. Radiation and Isotopes* **44**, 243–252. □

<sup>a</sup>Department of Archaeology and Natural History, Research School of Pacific and Asian Studies, Australian National University, Canberra ACT 0200, Australia.

<sup>b</sup>Research School of Earth Sciences, Australian National University.

<sup>c</sup>Transvaal Museum, P.O. Box 413, Pretoria 0001, South Africa.

\*Author for correspondence.

E-mail: bio\_anthropology@telstra.com

